Journal of Mines, Metals and Fuels, *72(2): 127-145; 2024. DOI: 10.18311/jmmf/2024/36463*

Print ISSN : 0022-2755

Journal of Mines, Metals and Fuels

Contents available at: *www.informaticsjournals.com/index.php/jmmf*

Analysing Slope Stability in Response to Blast-Induced Dynamic Loading by Pseudo-Static Approach

Ch. Venkat Ramana[1]*, N. R. Thote[1] and Arun Kumar Singh[2]

[1]Department of Mining Engineering, Visvesvaraya National Institute of Technology, Nagpur - 440010, India; ramanavnit@gmail.com

[2]Department of Mechanical Engineering, Visvesvaraya National Institute of Technology, Nagpur - 440010, India

Abstract

Regular blasting in opencast coal mines generates significant ground vibrations, impacting mine slope stability and posing risks to life and property. This study focuses on monitoring ground vibrations in an opencast coal mine through near-field monitoring and investigating the impact of blast-induced seismic loading on slope stability. The approach involves a pseudo-static method utilising Strength Reduction Factor (SRF), based on Finite Element (FE) numerical modelling software. The study examines a pit slope with a tension crack under seismic loading, varying the intensity of seismic coefficients (K_s) from 0 to 0.5. These coefficients are determined through field vibration monitoring during production blasts. In numerical modelling, seismic loading is considered in both horizontal (outward of slope face) and vertically downward (in-line with gravity) directions. Numerical modelling incorporates dimensionless horizontal seismic coefficient (K_h) and vertical seismic coefficient (K_v), and both directions which is expressed as Seismic Coefficient Ratio (SCR) which is the ratio of K_v and K_h for interpretation of results. Although SCR induces changes in the Factor of Safety (FoS), its impact is minimal compared to seismic loading solely in the horizontal direction. Consequently, increasing SCR leads to a decrease in FoS. The study observes that Peak Ground acceleration (PGA) in the longitudinal direction has greater dominance than in the transverse direction. Additionally, the seismic wave in the horizontal direction destabilises the slope more than the corresponding vertical seismic wave. These findings are elucidated in the context of the Critical Slip Surface (CSS).

Keywords: *Blasting, Critical Slip Surface, Near Field Monitoring, Pseudo-Static Approach, Seismic Coefficient, Seismic Coefficient Ratio, Slope Stability*

1.0 Introduction

Explosive blasting is a routine practice in open-pit mines to break down coal and overburden rocks[1-5]. Approximately 20-30 % of the explosive energy is dedicated to rock fragmentation, with the remaining energy dissipated as ground vibration, fly rock, air vibration and noise[4,6,7]. Ground vibration, a common by-product of blasting, is known to contribute to slope failures in open-cast mines[4,8-10]. Blasting is often treated as a dynamic analysis and besides geological and geotechnical factors, the dynamic loading resulting from blasting plays a significant role in slope stability by compromising the structural integrity of the slope[11].

Traditional methods for analysing slope stability under dynamic conditions include pseudo-static analysis, newmark displacement analysis and dynamic numerical analysis[1,12-14]. However, pseudo-static stability analysis primarily relies on the limit equilibrium method, where the impact of the dynamic load is assessed using a

*Author for correspondence

constant equivalent-static acceleration[1,15,16]. Existing literature predominantly focuses on the influence of horizontal seismic acceleration on slope stability with limited attention given to the effects of vertical acceleration on slope failures[15-21]. In the study conducted by Zhang *et al*., the impact of vertical acceleration on the stability of three-dimensional homogeneous slopes was explored[22]. Their findings suggested that the critical vertical seismic acceleration, acting against the slope's gravity can be disregarded if its value is less than half of the horizontal seismic acceleration. However, they underscored the significance of the vertical seismic coefficient in influencing slope stability. Shafiei *et al*.,[23] also investigated the effects of earthquakes and blasting on open-pit mine slopes, considering peak vertical and horizontal accelerations of 0.55g (K_v = 0.55) and 0.75g (K_h=0.75) respectively. Seismic coefficients, expressed as fractions of the acceleration due to gravity, play a crucial role in such analyses[1,12].

Li *et al.,*[24] conducted a static and pseudo-static assessment of three-dimensional slopes with cracks, applying horizontal seismic coefficients. Their findings indicated a reduction in slope stability due to the combined impact of cracks and seismic effects. However, they also observed that the three-dimensional effect enhanced slope stability. The study highlighted that cracks become a more dominant factor in slope failure at higher inclination angles and reduced cohesion. Additionally, the static and dynamic stability of the three-dimensional slopes in the presence of cracks was reported by He *et al*.,[25] considering face, toe and base failures. The nature of failure shifted from toe to face or base failure with an increase in the magnitude of the seismic coefficient. Moreover, only few researchers (Liu *et al*.,) studied the dynamic response characteristics and failure mechanisms of coal slopes containing weak intercalated layers under blasting loads. Furthermore, research on the factor of safety and critical slip surface was conducted by Li *et al.,*[24] Utili and Abd[26] analytically examined slope stability in the presence of fissures, considering both horizontal and vertical accelerations.

Ramana *et al*.,[5] recently conducted a numerical study examining the impact of the inclination angle of a tension crack on the stability of a rock slope. Their findings revealed that the FoS initially increases with the inclination angle of the tension crack until it reaches a constant value. However, a further increase in the inclination angle results in a decrease in FoS. The observed trend was explained by analysing the variation of corresponding shear stress at the location of crack nucleation zone of slope with a tension crack. Building on these insights, the current study aims to expand the analysis to include the presence of dynamic loads induced by blasting. The research involves monitoring ground vibrations in opencast mines and investigating the impact of dynamic loading due to blast vibrations on the stability of a slope with a tension crack. The analysis is conducted through pseudo-static analysis utilising RS2 Software, Finite Element Method (FEM) based numerical modelling software.

2. Location and Design Parameters of Opencast Coal Mines

The study site was situated in an Opencast Coal (OC) mine, centrally located in the Godavari Valley coalfield, India. The quarry's average length along the strike direction and average width along the dip-rise direction were recorded at 2.61km and 0.97km, respectively. The depth of the quarry varied, ranging from 30m at the rise side to 220m at the dip side. The mine maintains an annual coal production of 1.8 million tonnes, operating with a stripping ratio of 1:14. The total extractable coal reserve within this mine is estimated at 23.34 million tonnes, and the anticipated mine lifespan is 12 years. Figure 1 provides a panoramic view of pit slope benches and the workings of the OC mine. The mine adopts the benching method, deploying a shovel-dumper combination where individual benches in hard rock are inclined at an angle of 70°. The maximum height of these benches is restricted to 10m, with a berm width of 5m as depicted in Figure 2.

2.1 Geological Condition of Mine

Geological exploration of the quarry area in the studied opencast coal mine has unveiled a composition primarily characterised by medium to coarse-grained greyish-white sandstone. Within this geological context, 11 correlatable coal seams or horizons have been identified,



Figure 1. Panoramic view of pit slope benches and workings in opencast coal mine.

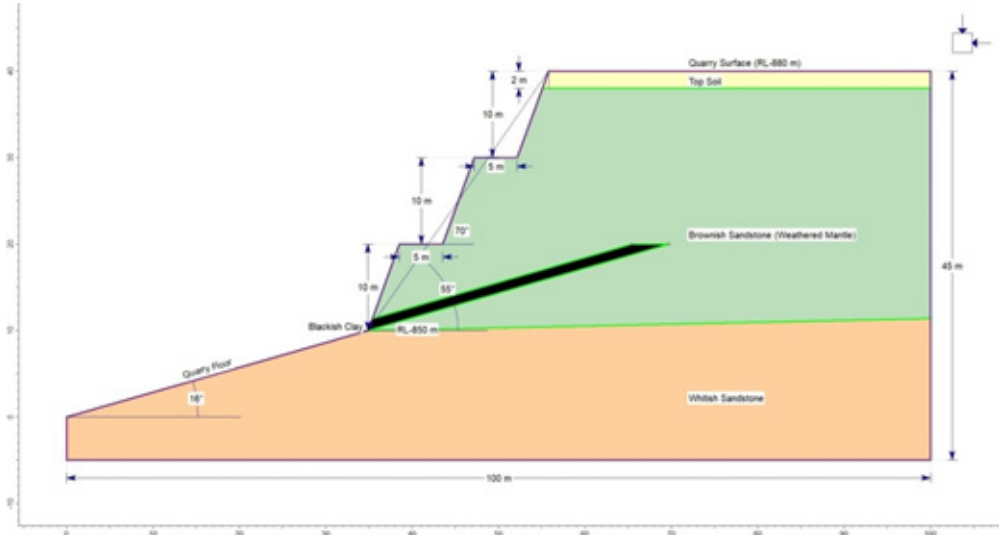


Figure 2. Graphical view of highwall bench configurations (Individual bench height-10m, width-5m, overall slope angle-55^0)

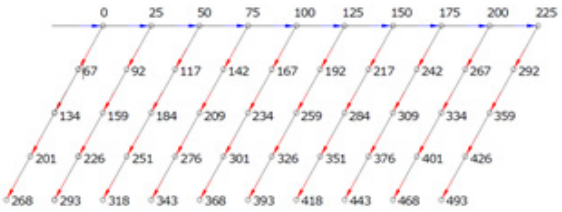
accompanied by subordinate clays and shale. These geological formations belong to the Barakar formation of the lower Gondwana group, representing the Permian age. The overburden, extending up to a depth of 30 meters from the surface, comprises of unconsolidated weathered mantle consisting mainly of sandstone, sandy clay and carbonaceous clay. The overall trend of the coal measures follows a direction from N40°W to S40°E, with a corresponding dip towards the northeast ranging between 12° and 16°. Notably, the block is characterised by a minimal presence of faults.

2.2 Drilling and Blasting Practices at Opencast Coal Mine

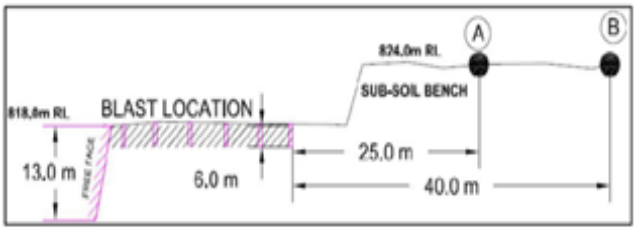
Blast holes, each with a diameter of 150 mm were strategically drilled in a staggered pattern with a spacing range of 5m to 6m and a burden varying between 4m to 5m. Due to equipment limitations, the depth of blast holes in overburden benches is maintained between 5m to 6m. Figure 3(a) offers a visual representation of a production blast in the opencast mine where approximately 500 to 600 blast holes are detonated daily, resulting in the



(a)



(b)



(c)

Figure 3. **(a)** A view of an opencast coal mine's production blasting, **(b)** A Typical blast's firing initiation sequence with non-electric delays (values are in milliseconds) **(c)** Schematic view showing the location of multi-hole production blast and vibration monitoring seismographs (A and B).

excavation of overburden reaching up to 50,000. The blasts are executed using Site-Mixed Emulsion (SME) explosives characterised by a Detonation Velocity (VOD) ranging between 4000 to 4500m/sec. Non-Electric Detonators (NONEL) are employed for both in-hole and surface hole-to-hole initiation. All blast holes are initiated at the bottom, employing a delay of 250ms. For hole-to-hole initiation within a row, a delay of 67ms is applied, while for row-to-row initiation, a delay of 25ms is utilised. Figure 3(b) illustrates a typical firing sequence diagram for blast holes with NONEL initiation. Figure 3(c) provides a schematic view indicating the typical location of the blast site and the placement of seismographs for the purpose of vibration monitoring during multi-hole production blasts in the opencast coal mine.

2.3 Monitoring and Analysis of Blast Vibrations

In the pursuit of conducting a pseudo-static stability analysis for a mining slope, acceleration-time records from twenty-three production blasts were monitored in the opencast coal mine. The blasts featured varying numbers of blast holes, ranging from 90 to 180. Monitoring distances spanned from 25m to 150m with a constant Maximum Charge per Delay (MCD) set at 120kg. The field measurements were executed using the Seismograph (Figure 4(a)). This instrument is equipped with a three-axis transducer, capable of detecting ground vibrations in three orthogonal directions: transversal, vertical and longitudinal (Figure 4(b)). For each blast, the peak particle velocity, peak acceleration and dominant

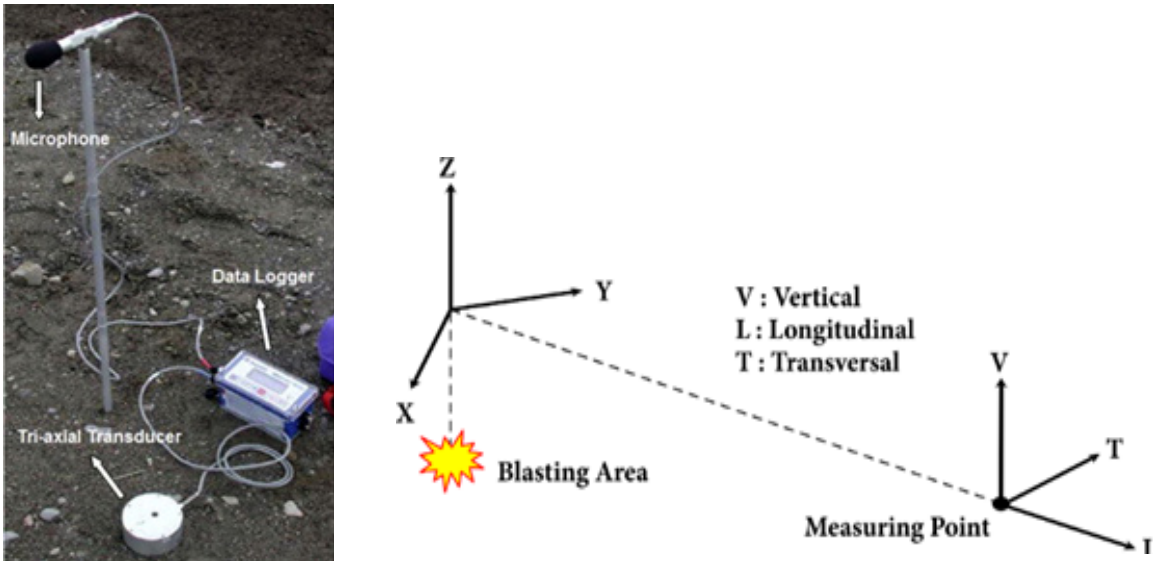


Figure 4. **(a)** A view of seismograph for near-field blast vibration monitoring, **(b)** Schematic diagram illustrating directions of blast-induced ground vibrations (adapted from Lee *et al.*[28]).

frequency at the maximum particle velocity were recorded for all three orthogonal directions and are presented in Table 1. The geophones used for measurements were accurately oriented towards the direction of the blast. Subsequently, Fast Fourier Transform (FFT) analysis of all vibrations was carried out using blast-induced analysis software "Blastware" from Instantel, Ottawa, ON, Canada[27].

2.4 Insights from Event and Fast Fourier Transform (FFT) Reports

Based on the field observations of blast vibrations detailed

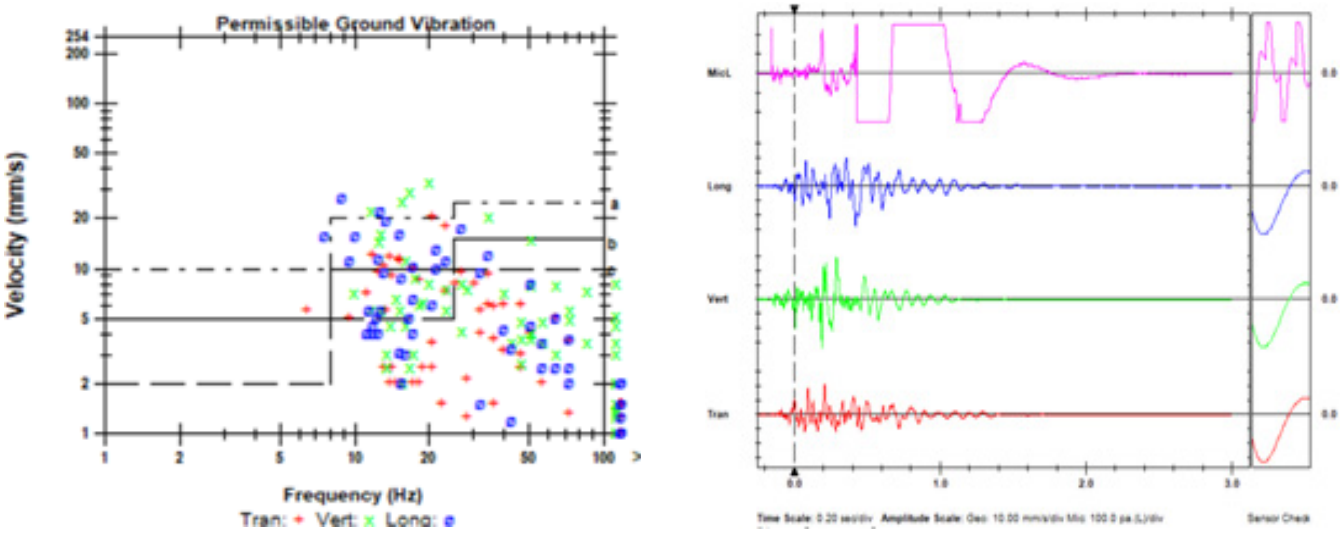


Figure 5. Typical event report of multi-hole production blast showing **(a)** PPV vs. frequency history, **(b)** PPV vs. time history in transverse, vertical and longitudinal directions.

Table 1. Near-field vibration monitoring results and estimated seismic coefficients from production blasts

B.N	MCD	D	SD	PPV			Frequency (Hz)			PGA (X 9.81 m/sec^2)			Seismic Coefficient	
				T	V	L	T	V	L	T	V	L	H	V
1	120	100	9.13	15.00	22.90	24.90	18.50	18.30	19.50	0.21	0.29	0.32	0.16	0.15
2	120	80	7.30	30.50	24.60	21.30	13.30	14.50	21.80	0.48	0.93	0.61	0.31	0.46
3	120	90	8.22	12.20	12.20	28.40	13.30	13.00	19.30	0.38	0.24	0.80	0.40	0.12
4	120	25	2.28	43.70	85.30	87.40	14.50	19.00	11.00	0.63	1.80	2.86	1.43	0.90
5	120	20	1.83	72.10	81.30	47.80	8.75	13.00	13.00	1.54	3.08	1.64	0.82	1.54
6	120	45	4.11	49.80	59.90	45.70	8.50	11.30	7.00	1.48	0.58	0.32	0.74	0.29
7	120	80	7.30	15.70	21.80	32.50	7.00	6.25	5.00	0.27	0.49	0.37	0.19	0.25
8	120	70	6.39	20.80	33.50	27.40	10.00	15.00	5.00	0.32	0.90	0.32	0.16	0.45
9	120	90	8.22	18.00	21.60	22.10	8.00	12.50	10.00	0.24	0.29	0.27	0.13	0.15
10	120	80	7.30	20.80	23.90	28.40	13.80	14.50	10.30	0.42	0.58	0.53	0.27	0.29
11	120	100	9.13	22.40	6.86	21.10	11.50	6.25	12.00	0.85	0.20	0.25	0.42	0.10
12	120	120	10.95	16.50	8.38	17.50	10.00	7.50	8.75	0.12	0.11	0.16	0.08	0.05
13	120	150	13.69	11.70	9.65	18.30	11.30	9.25	11.30	0.40	0.37	0.77	0.38	0.19
14	120	35	3.20	39.60	62.00	44.70	2.75	2.75	2.00	1.33	2.55	0.48	0.67	1.28
15	120	50	4.56	42.70	11.20	49.80	2.25	5.75	3.25	0.80	0.45	0.32	0.40	0.23
16	120	70	6.39	32.50	13.00	36.60	21.00	19.30	20.50	0.42	0.53	0.48	0.24	0.27
17	120	45	4.11	12.20	20.80	22.90	17.30	15.00	15.00	0.48	1.17	0.70	0.35	0.59
18	120	80	7.30	10.70	18.50	22.90	10.00	9.00	9.75	0.19	0.24	0.18	0.09	0.12
19	120	45	4.11	19.80	38.60	33.50	5.50	5.50	5.25	0.32	1.59	0.58	0.29	0.80
20	120	60	5.48	21.80	23.90	30.50	8.00	5.25	5.25	0.42	0.50	0.37	0.21	0.25
21	120	80	7.30	19.80	10.20	35.60	10.60	9.63	14.00	0.21	0.16	0.37	0.19	0.08
22	120	100	9.13	5.59	19.10	16.30	18.10	13.60	13.30	0.08	0.41	0.33	0.17	0.21
23	120	120	10.95	6.86	18.30	14.20	13.00	33.00	16.00	0.11	0.49	0.21	0.11	0.25

B.N: Blast number, MCD: Maximum charge per delay (kg), D: Distance (m), SD: Scaled distance , PPV: Peak Particle Velocity (mm/sec), PGA: Peak Ground Acceleration, T: Transverse direction, V: Vertical direction, L: Longitudinal direction, H: Horizontal direction.

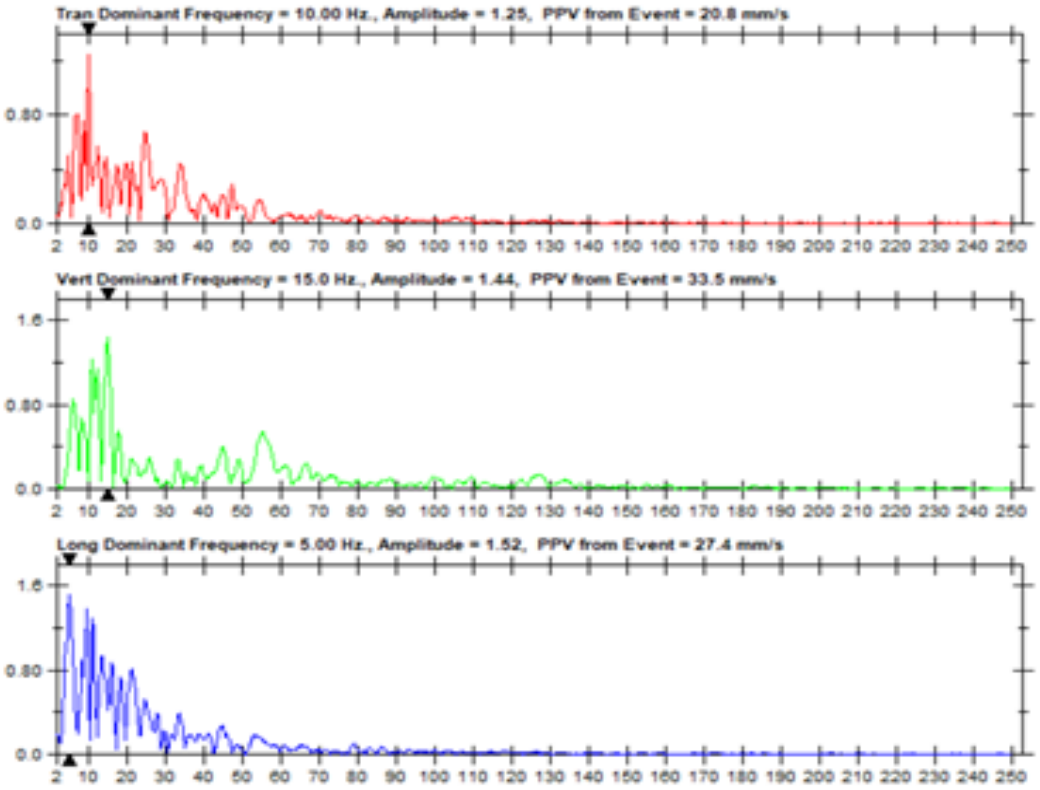


Figure 5c. FFT report for a typical multi-hole production blast (Blast No. 8), depicting the vibration and dominant frequency history in transverse, vertical, and longitudinal directions.

in Table 1 and subsequent analysis of the events recorded in the seismograph logger, it is observed that Peak Particle Velocity (PPV) and corresponding PGA occur at one time during the period of ground shaking due to blasting. Figure 5(a) presents a standard event report displaying the correlation between PPV and frequency, while Figure 5(b) illustrates the PPV versus time history. Additionally, Figure 5(c) showcases the FFT report, highlighting the dominant frequency of PPV in the transverse, vertical and longitudinal directions for a typical multi-hole production blast (Blast No.8).

From field monitoring of blast vibrations (Table 1), it is observed that PGA in the longitudinal direction is more dominant than in the transverse direction. Out of a total of 23 blast vibration measurements, 13 observations (56.5%) exhibit a more dominant PGA in the vertical direction, while 10 observations (43.5%) indicate a more dominant PGA in the horizontal direction (transverse and longitudinal combined). However, it is noteworthy that if blasting were conducted beneath the slope, higher PPV and PGA in vertical directions would be expected.

2.5 Estimation of Seismic Coefficients

The peak ground acceleration occurs one time during blasting. The seismic coefficient k_s values are presented in Table 1 and represent an average over the entire mass of the slope. Typically, the value of (k_s) is less than and never exceeds the PGA divided by gravity (g). In pseudo-static slope stability analysis, the selection of the seismic coefficient value is crucial, as highlighted by Melo and Sharma[12]. It is deemed reasonable to use a value of k_s is equal to 50% of the design PGA, in conjunction

with a pseudo-static factor of safety ranging from 1.0 to 1.2, particularly when the slope lacks definite planes of weakness[1]. In our study, we have also estimated the seismic coefficients for each blast by assuming them to be equal to 50% of the PGA.

2.6 Vibration Attenuation and Regression Analysis for Predicting Blast-Induced Ground Vibration

The attenuation law of blasting vibration is intricate, spanning disciplines such as explosion mechanics, wave

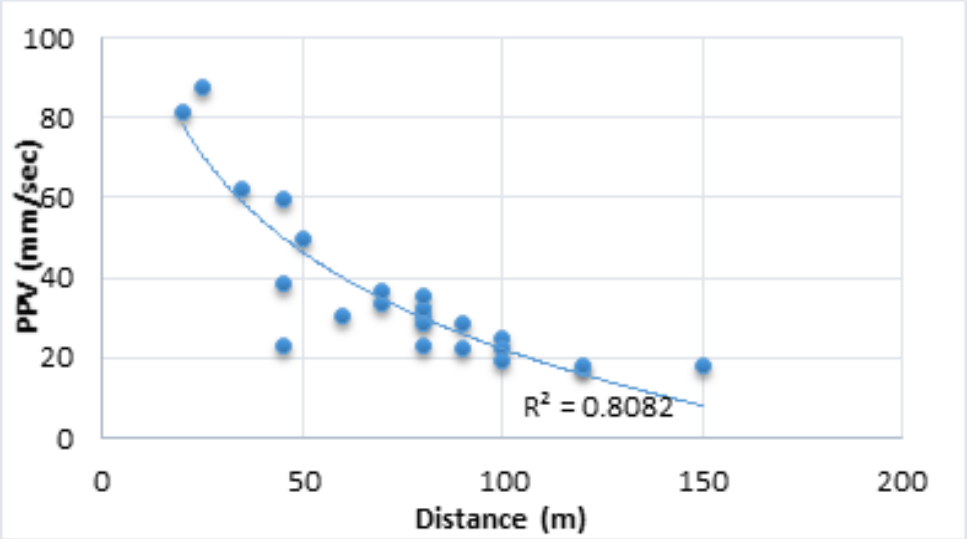


Figure 6a. Graph illustrating the attenuation of PPV with distance.

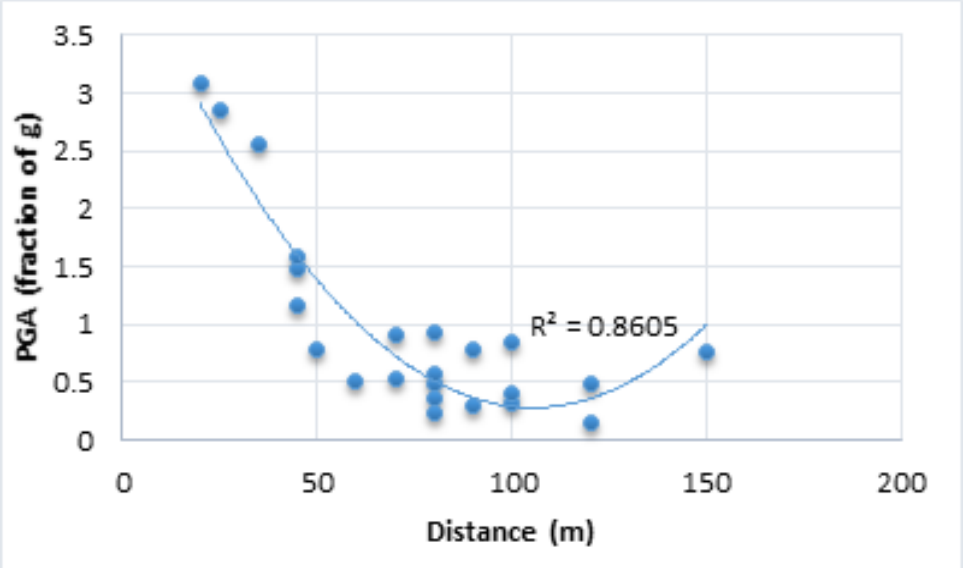


Figure 6b. Graph illustrating the attenuation of PGA with distance.

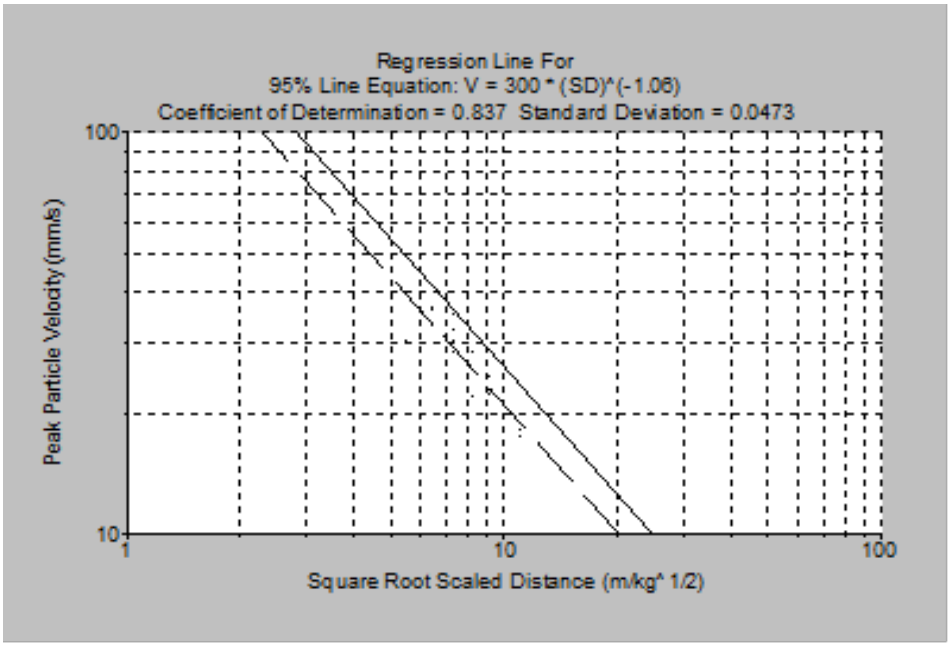


Figure 6c. Regression graph of PPV vs. scaled distance.

dynamics, rock mechanics, and geological engineering. Presently, accurate theoretical prediction methods are lacking. Instead, an effective approach involves empirical equation establishment through regression analysis of extensive measured data for both generation and attenuation of blasting vibration. Typically, PPV is chosen as the vibration variable. Several researchers have developed various empirical equations[29]. The vibration attenuation graph in blasting is crucial for several reasons. It helps to predict how blast-induced vibrations propagate through the ground over distance. This prediction is vital for assessing potential impacts on nearby structures (including pit slopes), utilities and the environment. It also provides critical data for regulatory compliance, risk management, optimisation, and effective communication with stakeholders[30]. The graphs illustrating the attenuation of PPV and PPA with distance for the blast vibration data as shown in Table 1 are depicted in Figure 6(a) and (b).

Pal Roy *et al.*,[31] explain that blast vibration analysis involves establishing a predictor equation derived from recorded vibrations, incorporating the distance between the blasting source and monitoring points, as well as the explosive charge per delay. The square root scaled distance regression analysis concept, developed by the United States Bureau of Mines (USBM), is widely employed for surface blasting in mines where ground vibration measurements are conducted on the surface[32]. This Scaled Distance (SD) is defined as $SD = D/\sqrt{Q}$, where, D is the distance between the blast location and the vibration monitoring station (m), and Q is the maximum charge per delay. The peak particle velocity PPV is determined by the following equation[27,33-37].

$$PPV = k(SD)^n$$

The constants k and n in the above equation are site-specific and depend on geological factors. Thus, the unit of SD is m/kg$^{0.5}$. The log-log graph depicting the best-fit straight line for Peak Particle Velocity (PPV) versus distance has a negative slope represented by n and an intercept denoted with k. Figure 6(c) illustrates the graph (regression line with a 95% confidence line) plotted on a log-log scale for the vibration data recorded from multi-hole production blasts against the corresponding scaled distance. The resulting scaled distance regression equation is as follows:

$$PPV = 300(SD)^{-1.06}$$

Utilising the aforementioned equation, PPV values are predicted in the mine for various distances and varying maximum charges per delay. It is notable that PPV diminishes with radial distance from the blasting site.

3. Pseudostatic Stability Analysis of Pit Slope Considering Blast Dynamic Load

The blast vibration wave is sinusoidal and seismic forces act in four directions on the slope face. However, in this study pseudo-static seismic forces due to blasting, expressed in terms of seismic coefficients are assumed to act in three different scenarios: (i) horizontally outward from the slope in the direction of failure, (ii) vertically downward in line with gravity, and (iii) both directions - horizontally outward from the slope and vertically downward. This approach is in line with the work of Bray, J.D., and Travasarou, T[13]. Figure. 7 illustrates a schematic diagram depicting the directions of seismic forces considered in the present pseudo-static slope stability analysis. Extending the current numerical simulation to incorporate actual blasts conducted in opencast coal mines would add valuable insights. Moreover, in real-world scenarios, blasting typically occurs away from the slope, often at the same or lower levels.

As stated earlier, the seismic coefficient in the horizontal direction is estimated as equivalent to 50% of the maximum value of PGA among the PGA in transverse and longitudinal directions, whichever is higher. Based on field blast vibration data, the observed seismic coefficient in the horizontal direction ranges from 0.11 to 0.42, while in the vertical direction, it varies from 0.05 to 0.46 for blasts conducted beyond 50m from pit slope benches (Table 1). The seismic coefficient values are found to range from 0.05 to 0.46. Considering this variability, the same seismic coefficient values (ranging from 0.1 to 0.5) have been applied in the present pseudo-static slope stability analysis, accounting for dynamic loads from production blasts conducted at a distance beyond 50m from pit slopes.

Pseudo-static stability analysis, employing constant equivalent-static acceleration, is a widely adopted method for assessing the impact of dynamic loading. In this analysis, the influence of blast loading is examined as seismic loading. Previous research has predominantly focused on seismic acceleration in the horizontal direction

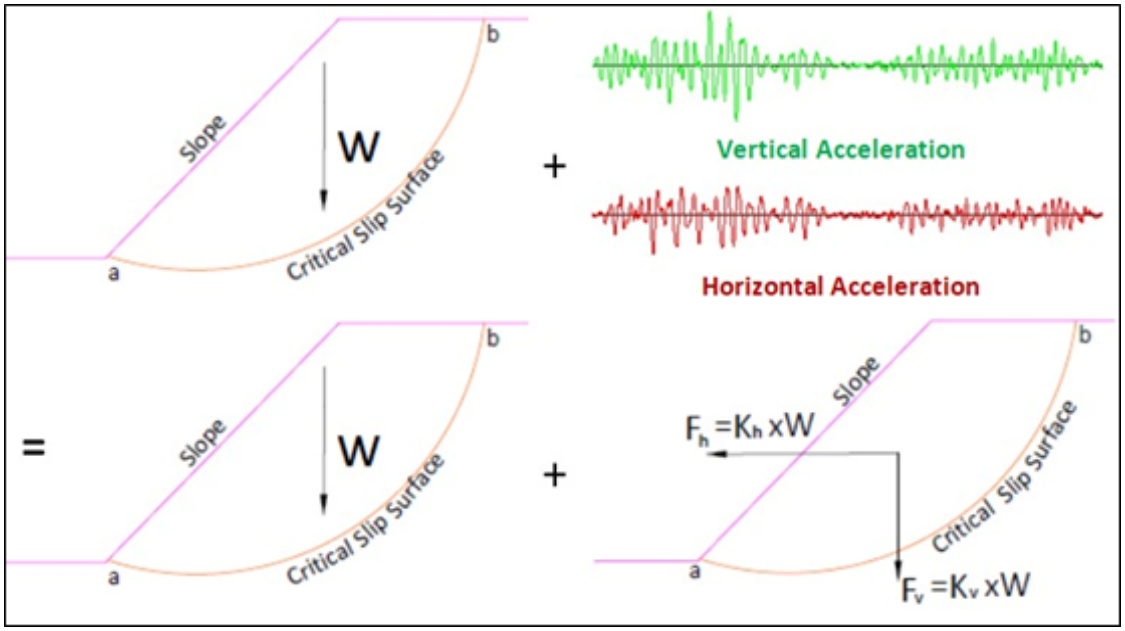


Figure 7. Seismic force directions considered in pseudo-static slope stability analysis with dynamic loading from production blasts.

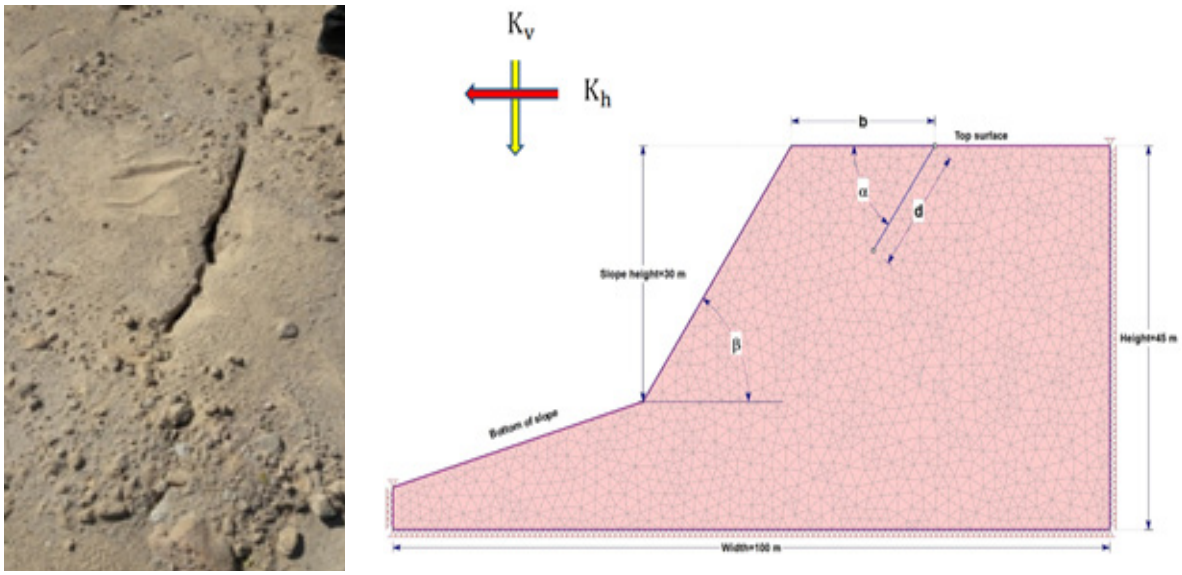
outward from the slope face. However, the present study delves into the effects of both horizontal and vertical PGA resulting from blasting on slope failures. It is assumed that blast holes do not intersect the Tension Crack (TC) and the blast position is situated elsewhere in the mine, causing vibration forces in the slope model. Additionally, it is assumed that the blast wave propagates horizontally outward from the slope face, vertically downward, and in both directions. Under these seismic loading conditions due to blasting, the stability analysis of the slope with a TC is conducted using FEM-based numerical modelling software. The assumption is made that blasting occurs beneath the slope, and the slope is considered fully drained.

3.1 Development of Slope Model and Characterisation of Rock Mass Properties

We examined the impact of both horizontal and vertical acceleration resulting from blasting on the stability of a slope with a TC. Furthermore, our interest extends to investigating the effects of horizontal and vertical acceleration on the CSS. This study proves valuable in assessing the magnitude of hazards and understanding the behaviour of the critical slip surface in slope failures induced by blasting. The typical view of a tension crack at the crest of the slope is depicted in Figure 8(a). The findings of this study contribute to seismic slope stability analysis with seismic coefficients up to 0.5, considering mine production blasts conducted at a distance of 50 to 150m from the pit slope with a Maximum explosive Charge per Delay (MCD) of 120 kg.

Figure 8(b) illustrates a representative slope model with a tension crack based on field conditions. Figures 1 and 2 present a schematic view of the highwall bench configurations in an opencast coal mine, featuring individual benches with a height of 10m and a width of 5m, maintaining an overall slope angle of 55^0. From this configuration, a typical slope model with a tension crack was developed, as shown in Figure 8(b). The two-dimensional slope model has dimensions of 100m width, 30m height, and a slope angle, $\beta=55^0$. It includes a TC with finite length (d = 9 m), an inclination angle (α), and a crest distance (b) of 10m.

The rock mass of the slope is assumed to be homogeneous and isotropic, possessing an elastic modulus of 0.15 GPa and a density of 22 kN/m^3. The analysis considers a hydrostatic stress field. The left, right and bottom boundaries of the slope model are restrained in both X and Y directions while the top, bottom and face boundaries are unrestrained in both X and Y directions,



(a) (b)

Figure 8. **(a)** Typical view of tension crack at the crest of slope in an opencast coal mine; **(b)** Numerical pit slope model with tension crack (k_h & k_v are seismic coefficients)

allowing for deformation. The numerical simulations employ the Mohr-Coulomb (MC) failure criterion with material properties including a cohesion of 85.0kPa and an angle of internal friction of 20 degrees. The slope model's domain is discretised with graded meshing using 6-noded triangular elements (T6). Further discretisation of the slope face region is accomplished with a uniform size of T6 elements, each with a side length of 1m, using advanced meshing options in *RS2* FEM software. The slope model comprises a total of 3382 elements and 6879 nodes. Additional details on the study, specifically the impact of an inclined TC on slope stability can be found in our prior paper[5]. The RS2 software is employed to ascertain the Critical Strength Reduction Factor (CSRF) and identify the CSS of the slope. The CSRF represents the FoS[16,20]. This software utilises the FEM in conjunction with the shear strength reduction method.

4. Results and Discussions

4.1 Impact of Seismic Loading Acting Horizontally Out of the Slope Face on Slope Stability

The results in Figure 9(a) present the variation of CSRF with inclination angle (α) of the TC for different horizontal seismic coefficients k_h= 0.1 to 0.5. At the same time, the vertical seismic coefficient was considered to be zero. It is observed that the magnitude of CSRF decreases upon an increase in k_h. The SCR in this case will be 0 as k_v=0. For instance, when k_h increased from 0.1 to 0.5, the magnitude of CSRF decreased from 1.03 to 0.63 when α= 90^0. However, this drop will also depend on the inclination angle of TC. We have also studied the corresponding variation of shear stress at the location of the shear zone around TC where failure is initiated as shown in Figure 9(b). There is not much variation of shear stress with an increase in k_h from 0.1 to 0.5. The CSS is also studied and the results in Figure10 show that the magnitude of the shear failure zone is increasing with an increase in k_h for the same inclination of TC. It is observed that the variation of shear stress shows the opposite trend compared to variation of CSRF vs. α. It is constant with α = 60°, 90°, 120° and CSRF drops again as α becomes 150°. If k_h is increased to 0.5, the magnitude of CSRF is almost constant for α=30°, 60°, 90°, 120° when α=150°, CSRF decreases further to 0.45.

With an increase in seismic coefficient in the horizontal direction out of the slope face, the CSRF reduces linearly and corresponding shear stress at the location of crack nucleation and along the CSS also increases and the magnitude of shear zone increases near the base of TC.

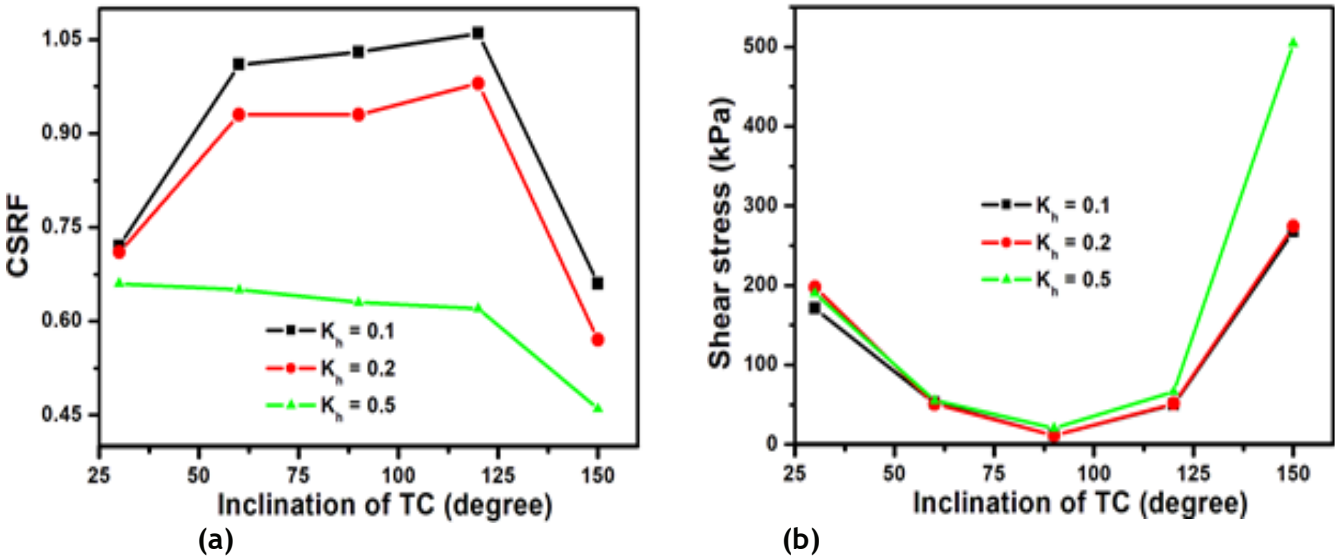


Figure 9. **(a)** Effect of the inclination angle (α) of TC on CSRF for different values of, **(b)** Corresponding variation of shear stress at the location of CSRF of slope with TC of length (d) = 9.0m at a fixed crest distance (b) = 10.0m.

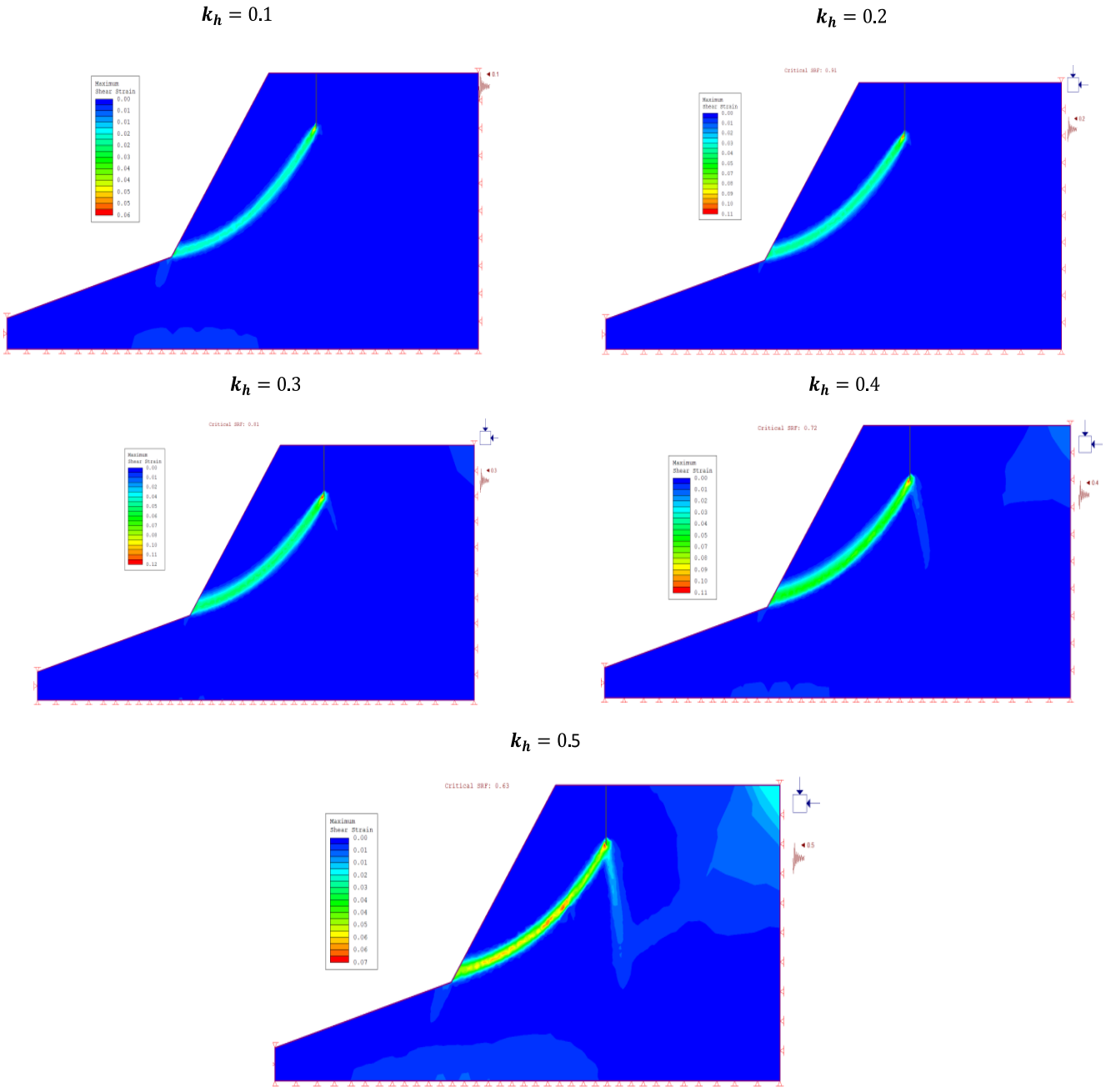


Figure 10. Critical slip surface plots of slope with a vertical TC for different values of k_h when k_v=0.

The CSS extends from the toe of the slope to the base of TC in all cases of SCR. When the magnitude of k_h > 0.3, the shear zone is observed to be extending to the bottom of slope from the base of TC.

4.2 Impact of Downward-Acting Seismic Load Due to Blasting on Slope Stability

The results in Figure 11(a) present the variation of CSRF with inclination angle (α)of the TC for different vertical

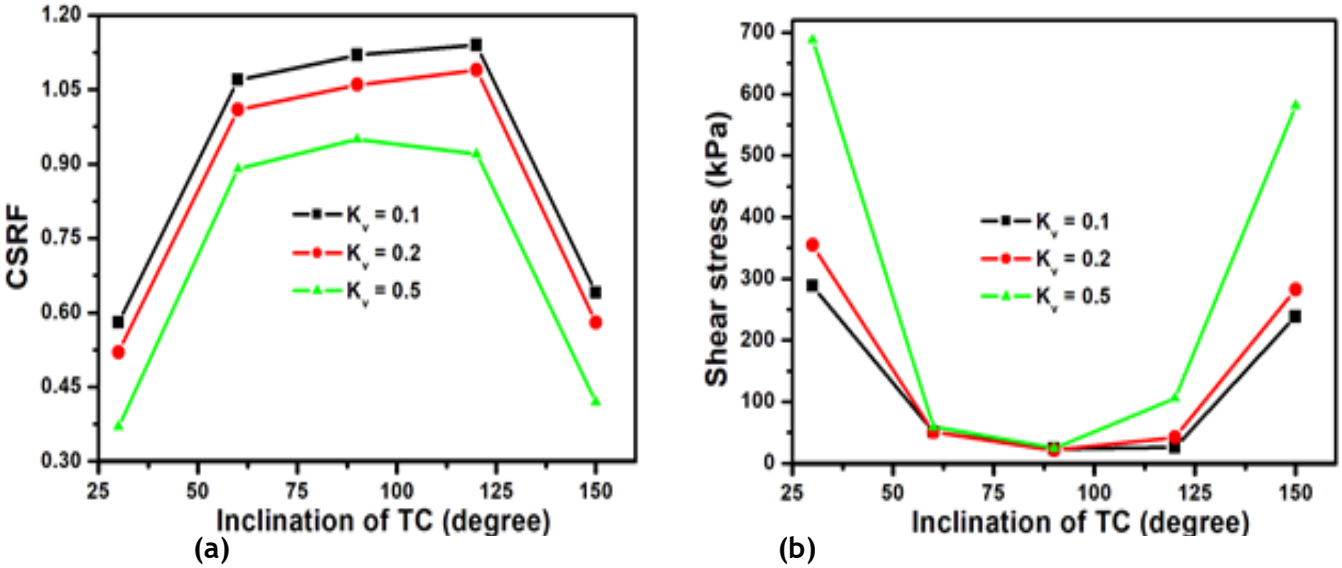


Figure 11. **(a)** Effect of the inclination angle (α) of TC on CSRF for different values of **(b)** Corresponding variation of shear stress at the location of CSRF of slope with TC of length (d) = 9.0m at a fixed crest distance (b) = 10.0m

seismic coefficients k_v= 0.1 to 0.5. At the same time, the horizontal seismic coefficient was considered to be zero. It is observed that the magnitude of CSRF decreases upon an increase in k_v . The SCR in this case will be infinite as k_h=0. For instance, when k_v increased from 0.1 to 0.5, the magnitude of CSRF decreased from 1.12 to 0.95 when α=90°.However, this drop will also depend on the inclination angle of TC. We have also studied the corresponding variation of shear stress at the location of the shear zone around TC where failure was initiated. Figure 11(b) depicts that there is much variation of shear stress with increase in k_v from 0.1 to 0.5 at α=30°&90°. The CSS is also studied and the results in Figure 12 shows that the magnitude failure zone is increasing with an increase in k_v for the same inclination of TC. With the increase in Seismic coefficient in vertically downward direction in line with gravity, the CSRF is reducing linearly and corresponding shear stress at the location of crack nucleation is increasing. Upon increasing k_v, the magnitude of shear zone is observed to remain constant located near the base of the TC. The corresponding CSS extends from the toe of the slope to the base of TC in all cases of k_v = 0.1 to 0.5. Moreover, k_h results in destabilising the slope more than k_v for the same seismic coefficient due to blasting.

The increase of the shear zone with an increase in K_v is observed to be less compared to the shear zone increase with increase in K_h. From Figure 13, it is observed that K_v is less influential on CSRF compared to K_h. For a slope with vertical TC and at a fixed value of the seismic coefficient, the magnitude of CSRF decreases from 8% to 34% when the seismic load acts in horizontal direction out of slope face than when seismic load acts in vertically downward direction. In other words, the CSRF of the slope increased by 9% to 51% when the seismic load acts in a vertically downward direction rather than in a horizontal direction out of the slope face.

4.3 Impact of Seismic Loading Simultaneously Acting in Both Horizontal and Vertical Directions on Slope Stability

In the dynamic stability analysis of rock slope, effect of the ratio of horizontal and vertical seismic coefficient (k_v/k_h) is investigated in present numerical simulations. The SCR=k_v/k_h was varied from 0 to 0.5 with an increment of 0.125. The value of horizontal seismic coefficient k_h is kept constant at 0.2 and the seismic load is assumed to act towards the slope face (excavation area) in the horizontal

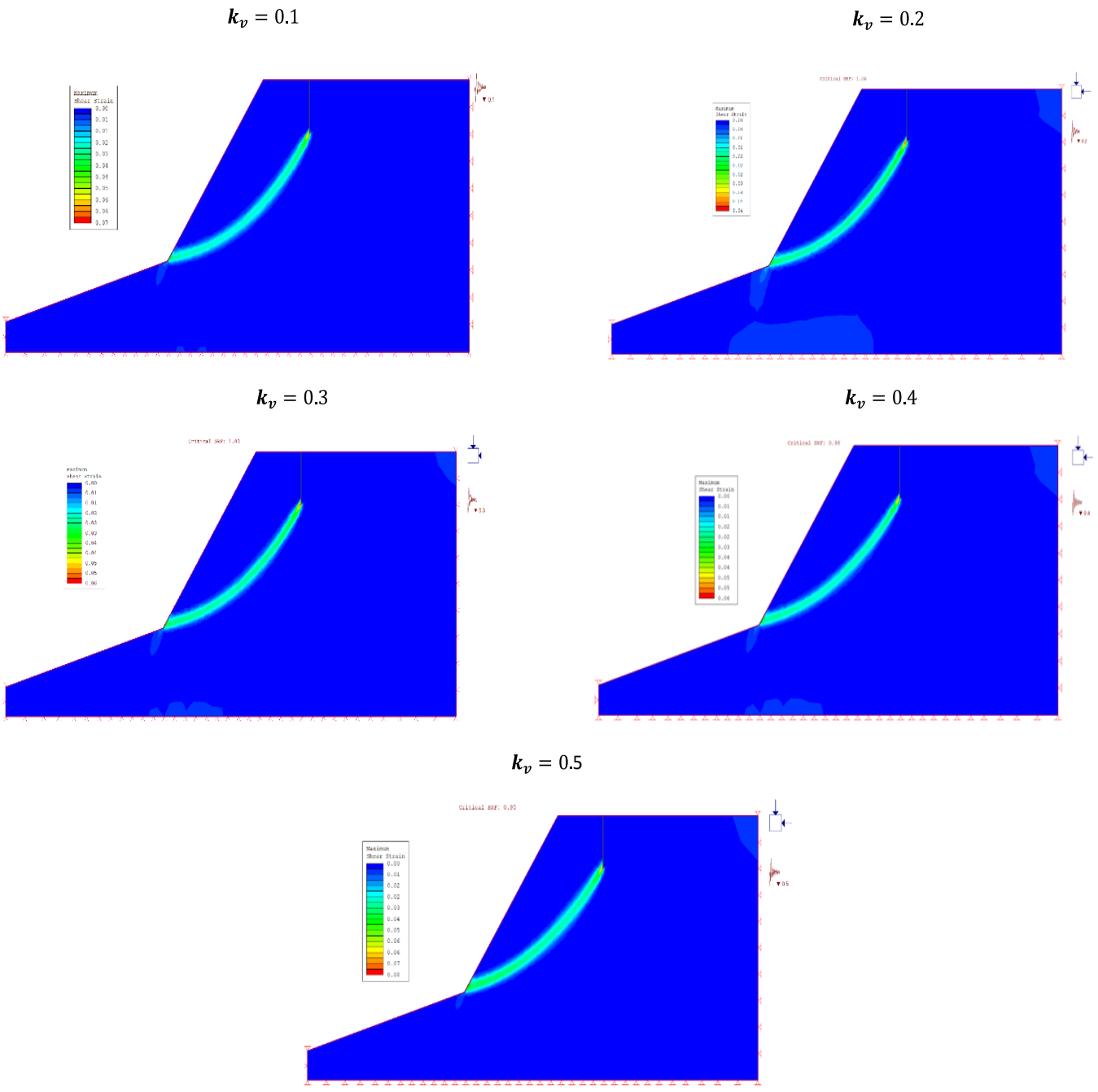


Figure 12. Critical slip surface plots of pit slope with TC for different values of k_v when k_h=0.

direction as these are the observed typical values of seismic coefficients in the field due to blasting.

It is concluded that SCR results in a decrease of FoS, however its effect is not very significant. Although SCR causes changes in FoS, the effect is very minimal for the fixed k_h. In other words, increasing the value of SCR results in decreasing CSRF. When k_h and k_v is considered, expressed as SCR (k_v/k_h), the CSRF is decreased by 2 to

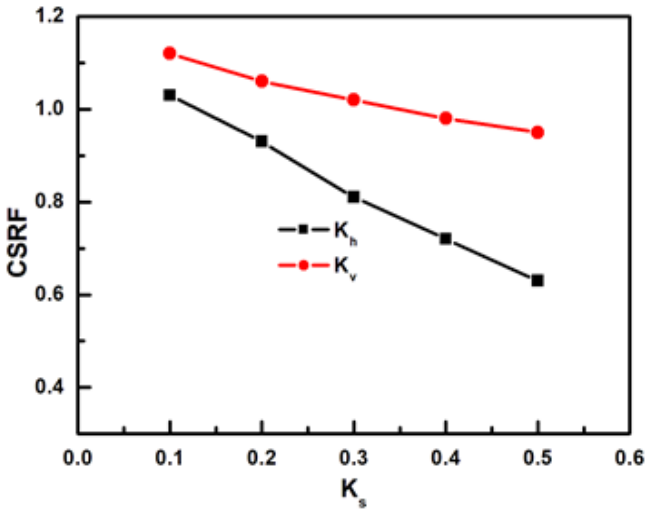


Figure 13. Effect of the seismic coefficient (K_s) i.e., K_h and K_v on CSRF of the slope with vertical TC (α=90⁰) of length (d) = 9.0m at a fixed crest distance (b) = 10.0m.

10% for different inclinations of TC as shown in Figure 14, compared to the analysis where kv is not considered i.e., (k_v/k_h=0). These results were matching with the published results available in literature[18,22].

The results in Figure 14 (a) depict the variation of FoS with the dip (α) of TC for different values of SCR. The ratio SCR varied from 0 to 0.5 with an increment of 0.125. The value of horizontal seismic coefficient k_h k was kept constant at 0.2. In the model, TC of length 9.0m is assumed and located at a crest distance 10.0m as in the previous two models. It is observed that for fixed SCR, CSRF increases slightly first with, after that remains constant with α = (60⁰, 90⁰ and 120⁰) and decreases further as α = 150⁰. For instance, fixed SCR = 0.125, the magnitude of CSRF is 0.75 when, it becomes almost constant at 0.90 for , CSRF becomes 0.6 when It is observed that k_v/k_h is not significant compared to dip of TC to cause instability of slope. The behaviour of CSS is presented in Figure15 With the increase in SCR, the magnitude of the shear zone is observed to be located near the base of TC. The CSS extends the slope to the base of TC in all cases of SCR = 0 to 0.5. The increase of the shear zone with an increase in SCR is observed to be less compared to the shear zone increase with the increase in k_h. The CSS's entry and exit points remain located at the base of TC and the Toe of the slope in all cases of SCR.

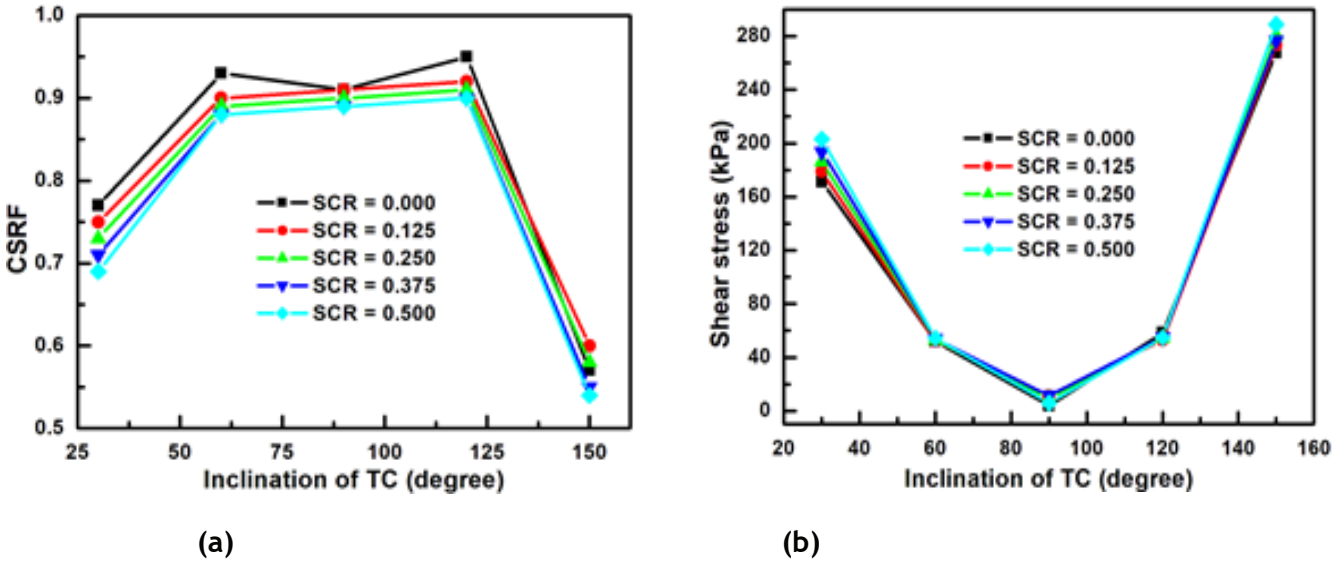


Figure 14. **(a)** Variation of FoS with a dip of TC for varying values of SCR; **(b)** Corresponding variation of shear stress.

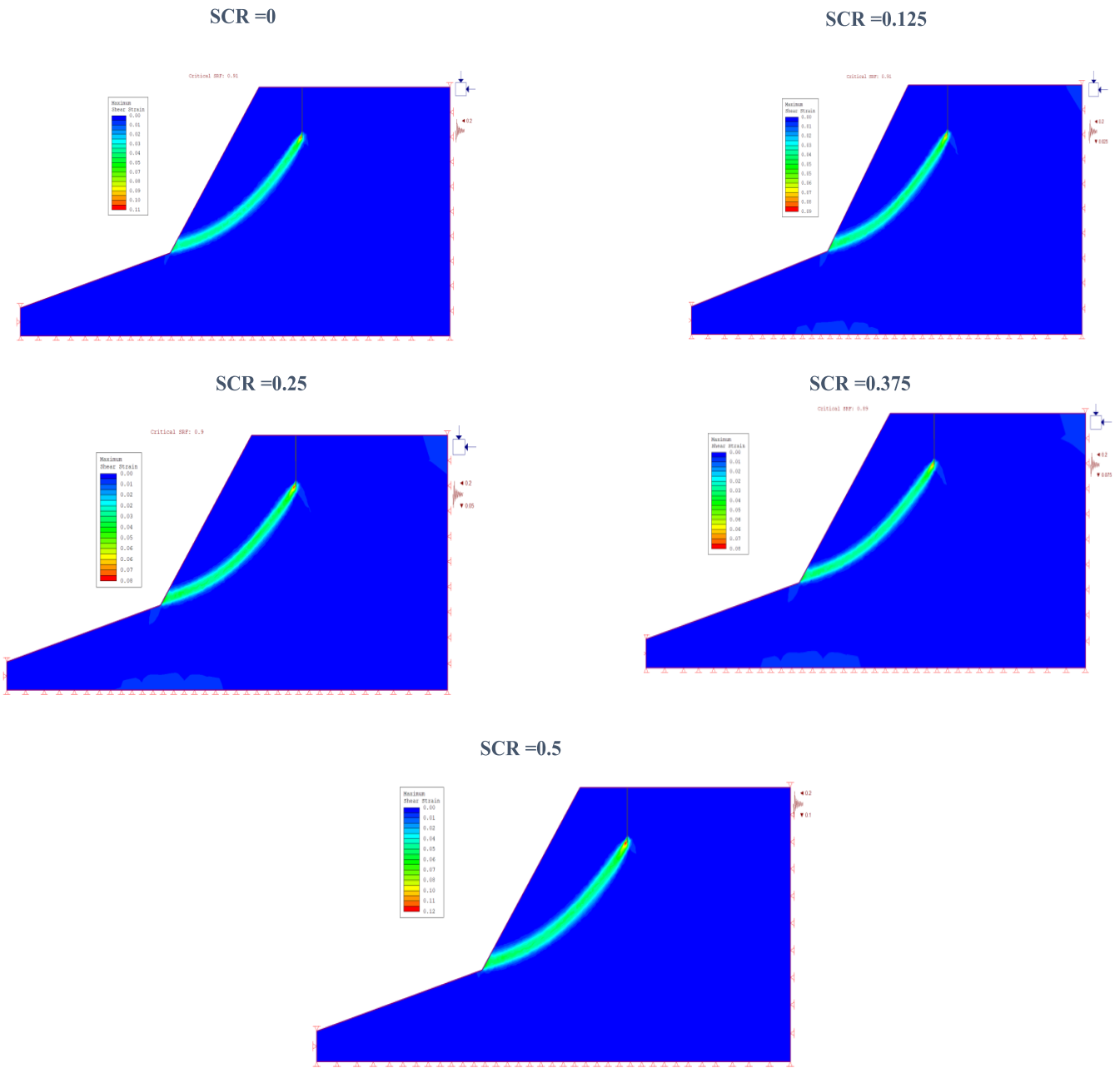


Figure 15. Critical Slip Surface (CSS) plots of slope for varying values of SCR when the value k_h=0.2.

5. Conclusions

The current numerical study establishes that the SCR has a minimal impact on the FoS, with an increasing SCR leading to a decreasing CSRF. Notably, the horizontal seismic coefficient k_h exerts a more influential effect on CSRF compared to the vertical seismic coefficient k_v in terms of slope stability. Analysing the critical slip surface,

it is observed that the shear zone is more significant for k_h than for k_v. Consequently, for the same level of PGA resulting from blasting, the PGA acting horizontally destabilises the slope more than the PGA acting vertically. Field blast vibration monitoring supports the conclusion that the PGA in the longitudinal direction is more dominant than in the transverse direction.

8. References

1. Wyllie DC, Mah C. Rock slope engineering. CRC Press; 2004.
2. Inumula S, Satyanarayana I, Budi G, Sen P, Sinha AK. Stability evaluation of highwall slope in an opencast coal mine- A case study. J Mines Metals Fuels. 2018; 66:209-17. https://doi.org/10.18280/mmc_c.780301
3. Ramana CV, Thote NR, Singh AK. Numerical investigation into factors affecting the stability of opencast coal mine's rise side highwall slope. J Mines Metals Fuels.2024; 72(1):71-81. https://doi.org/10.18311/jmmf/2024/36299
4. hote NR, Ramana CV. Investigation into the effect of blasting on slope stability in opencast coal mines. In Rock Fragmentation by Blasting: The 10th International Symposium on Rock Fragmentation by Blasting. Taylor and Francis Books Ltd. 2013; 10:763-8
5. Ramana CV, Thote NR, Singh AK. Effect of inclined tension crack on rock slope stability by SSR technique. Intelligent Automation and Soft Computing. 2023; 36(1). https://doi.org/10.32604/iasc.2023.031838
6. Kesimal A, Ercikdi B, Cihangir F. Environmental impacts of blast-induced acceleration on slope instability at a limestone quarry. Environmental Geology. 2008; 54:381-9. https://doi.org/10.1007/s00254-007-0825-4
7. Azizabadi HR, Mansouri H, Fouché O. Coupling of two methods, waveform superposition and numerical, to model blast vibration effect on slope stability in jointed rock masses. Computers and Geotechnics. 2014; 61:42-9. https://doi.org/10.1016/j.compgeo.2014.04.008
8. Deb D, Kaushik KN, Choi BH, Ryu CH, Jung YB, Sunwoo C. Stability assessment of a pit slope under blast loading: A case study of Pasir coal mine. Geotechnical and Geological Engineering. 2011; 29:419-29. https://doi.org/10.1007/s10706-010-9387-4
9. Jiang N, Zhou C, Lu S, Zhang Z. Propagation and prediction of blasting vibration on a slope in an open pit during underground mining. Tunnelling and Underground Space Technology. 2017; 70:409-21. https://doi.org/10.1016/j.tust.2017.09.005
10. Bazzi H, Noferesti H, Farhadian H. Modelling the effect of blast-induced vibrations on the stability of a faulted mine slope. Journal of the Southern African Institute of Mining and Metallurgy. 2020; 120(10):591-7. https://doi.org/10.17159/2411-9717/1066/2020
11. Wu T, Zhou C, Jiang N, Xia Y, Zhang Y. Stability analysis for high-steep slope subjected to repeated blasting vibration. Arabian Journal of Geosciences. 2020; 13:1-2. https://doi.org/10.1007/s12517-020-05857-y
12. Melo C, Sharma S. Seismic coefficients for pseudostatic slope analysis. In13th World Conference on Earthquake Engineering. Canada, Vancouver; 2004. p. 369.
13. Bray JD, Travasarou T. Pseudostatic coefficient for use in simplified seismic slope stability evaluation. Journal of Geotechnical and Geo-Environmental Engineering. 2009; 135(9):1336-40. https://doi.org/10.1061/(ASCE)GT.1943-5606.0000012
14. Bray JD, Travasarou T. Pseudostatic slope stability procedure. In 5th International Conference on Earthquake Geotechnical Engineering; 2011. p. 255-66.
15. Metya S, Chaudhary N, Sharma KK. Psuedostatic stability analysis of rock slope using Patton's shear criterion. International Journal of Geo-Engineering. 202; 12:1-22. https://doi.org/10.1186/s40703-020-00137-w
16. Sun C, Chai J, Luo T, Xu Z, Qin Y, Yuan X, Ma B. Stability charts for pseudostatic stability analysis of rock slopes using the nonlinear Hoek-Brown strength reduction technique. Advances in Civil Engineering. 2020; 3:1-6. https://doi.org/10.1155/2020/8841090
17. Li AJ, Lyamin AV, Merifield RS. Seismic rock slope stability charts based on limit analysis methods. Computers and Geotechnics. 2009; 36(1-2):135-48. https://doi.org/10.1016/j.compgeo.2008.01.004
18. Latha GM, Garaga A. Seismic stability analysis of a Himalayan rock slope. Rock Mechanics and Rock Engineering. 2010; 43:831-43. https://doi.org/10.1007/s00603-010-0088-3
19. Zhang Y, Zhang Y. Seismic slope stability analysis by considering tension crack. Earthquake-induced landslides: Initiation and run-out analysis by considering vertical seismic loading, tension failure and the trampoline effect. 2018: 41-62. https://doi.org/10.1007/978-981-10-2935-6_3
20. Sun C, Chai J, Ma B, Luo T, Gao Y, Qiu H. Stability charts for pseudostatic stability analysis of 3D homogeneous soil slopes using strength reduction finite element

method. Advances in Civil Engineering. 2020; 3:1-16. https://doi.org/10.1155/2019/6025698
21. Das S, Maheshwari BK. Effect of vertical seismic coefficient in slope stability analysis. In Indian Young Geotechnical Engineers Conference. Singapore: Springer Nature Singapore; 2019. p. 281-7. https://doi.org/10.1007/978-981-16-6456-4_30
22. Zhang F, Gao Y, Wu Y, Zhang N, Qiu Y. Effects of vertical seismic acceleration on 3D slope stability. Earthquake Engineering and Engineering Vibration. 2016; 15(3):487-94. https://doi.org/10.1007/s11803-016-0338-9
23. Ganjeh RS, Memarian H, Khosravi MH, Mojarab M. A comparison between effects of earthquake and blasting on the stability of mine slopes: A case study of Chadormalu open-pit mine. Journal of Mining and Environment. 2019; 10(1):223-40.
24. Li ZW, Yang XL, Li TZ. Static and seismic stability assessment of 3D slopes with cracks. Engineering Geology. 2020; 265:105450. https://doi.org/10.1016/j.enggeo.2019.105450
25. He Y, Yu J, Yuan R, Wang W, Nikitas N. Stability and failure mechanisms in three-dimensional cracked slope: Static and dynamic analysis. Computers and Geotechnics. 2022; 144:104626. https://doi.org/10.1016/j.compgeo.2021.104626
26. Utili S, Abd AH. On the stability of fissured slopes subject to seismic action. International Journal for Numerical and Analytical Methods in Geomechanics. 2016 ; 40(5):785-806. https://doi.org/10.1002/nag.2498
27. Stanković S, Katalinić M, Kuhinek D, Bohanek V. Detecting a typical value and their influence on blast-induced seismic measurement results. Applied Sciences. 2022; 12(12):5820. https://doi.org/10.3390/app12125820
28. Lee CW, Kim J, Kang GC. Full-scale tests for assessing blasting-induced vibration and noise. Shock and Vibration. 2018; (16):1-14. https://doi.org/10.1155/2018/9354349
29. Yu C, Li H, Yue H, Wang X, Xia X. A case study of blasting vibration attenuation based on wave component characteristics. Journal of Rock Mechanics and Geotechnical Engineering. 2023; 15(5):1298-311. https://doi.org/10.1016/j.jrmge.2022.09.013
30. Oyler S, Kertesz C, Bruce J. Blasting vibration control-overview of past practices and current trends. In: Proceedings of the 26th Annual Conference on Explosives and Blasting Technique. International Society of Explosives Engineers; 2000.
31. Roy PP. A comprehensive assessment of ground vibrations and structural damage caused by blasting. In Rock Fragmentation by Blasting. CRC Press; 2012. p. 453-62. https://doi.org/10.1201/b13759-60. PMid:22496088.
32. Duvall WI, Fogelson DE. Review of criteria for estimating damage to residences from blasting vibrations. US Department of the Interior, Bureau of Mines; 1962.
33. Dowding CH. Blast vibration monitoring and control: A thirty-year perspective. In ARMA US Rock Mechanics/Geomechanics Symposium. ARMA-99; 1999.
34. Agrawal H, Mishra AK. Modified scaled distance regression analysis approach for prediction of blast-induced ground vibration in multi-hole blasting. Journal of Rock Mechanics and Geotechnical Engineering. 2019; 11(1):202-7. https://doi.org/10.1016/j.jrmge.2018.07.004
35. Ainalis D, Kaufmann O, Tshibangu JP, Verlinden O, Kouroussis G. Modelling the source of blasting for the numerical simulation of blast-induced ground vibrations: A review. Rock Mechanics and Rock Engineering. 2017; 50:171-93. https://doi.org/10.1007/s00603-016-1101-2
36. Kong KW. Blasting vibration assessment of rock slopes and a case study. In Slope Stability 2013: Proceedings of the 2013 International Symposium on Slope Stability in Open Pit Mining and Civil Engineering. Australian Centre for Geomechanics; 2013. p. 1335-44. https://doi.org/10.36487/ACG_rep/1308_95_Kong
37. Matidza MI, Jianhua Z, Gang H, Mwangi AD. Assessment of blast-induced ground vibration at Jinduicheng molybdenum open pit mine. Natural Resources Research. 2020; 29:831-41. https://doi.org/10.1007/s11053-020-09623-5